ROTATIONAL PRECISION MEMS-BASED CLAMPING MECHANISM FOR STABLE FIXATION OF ELASTIC MECHANISMS

D.M. Brouwer, IMPACT Institute, University of Twente, the Netherlands

B.R. de Jong, M. J. de Boer, MESA+ Institute, University of Twente, the Netherlands

H.M.J.R. Soemers, Philips Applied Technologies, Eindhoven, the Netherlands

Abstract: *A mechanical clamp is presented which clamps one of the actuators of the MEMS-based TEM sample manipulator. The clamp incorporates a relatively large clamp force of 0.5 mN and is able to maintain the clamp force without external power. Although compliant mechanism design in MEMS design requires extra attention because of the relatively large deflections, small actuations forces and relatively large actuation stiffness, the real challenge lays in designing within the limited fabrication techniques. Though still in development, the fabrication technique proposed offers 35 μm high mechanisms with a trench width bandwidth of 3-20μm. The fabrication technique is compatible with the fabrication of a 6 Degree-of-freedom manipulator.*

Introduction

Conventional TEM sample manipulators often lack the crucial stability of 0.1 nm/min. A MEMS manipulator attached directly to the TEM pole would greatly increase both thermal and dynamic stability. However a stable E-beam requires no interference of electric or magnetic fields. Therefore the position of the manipulator should be maintained passively. To this end a mechanical clamp is presented which clamps one of the actuators of the MEMS-based TEM sample manipulator [1]. The clamp incorporates a relatively large clamp force of 0.5 mN and is able to maintain the clamp force without external power. A theoretical basis of the clamp has been presented in previous work [2]. In this paper the design and fabrication of a second generation rotational clamp is presented. This clamp design is part of a research project for a 6 Degrees-of-Freedom MEMS TEM sample manipulator.

Clamp design

Figure 1 shows part of the manipulator tail which has to be fixed in *y*-direction by the clamp mechanism. The clamp mechanism clamps the manipulator tail which is connected to the manipulator actuator shuttle. A transmission ratio is created to increase the clamp force and to decrease the influence of play in the rack and pin locking mechanism.

The operation of the total clamp mechanism starts by closing the parallel plate actuator. The pin moves down and the clamp shuttles are free to rotate around the pivots. The two jaws are actuated by one comb-drive collectively which results in a rotation of the jaws and shuttles around the pivots. Once a desired clamp force is established the parallel plate actuator is switched off and the pin is locked in one of the gaps of the rack. The comb-drive actuator can be switched off.

Figure 2 shows the clamp design. The jaw is suspended by leaf-springs *A* and *B*. In general, leaf-springs are very stiff in tensile direction while in bending direction they are compliant. When the two leaf-springs *A* and *B* deform together, the jaw will rotate around a virtual pivot which is the intersecting axis of leaf-springs *A* and *B*. The rotational comb operates at a larger radius than the jaw creating a force amplification. Leaf-springs *C* & *D* intersect at the same virtual pivot as leaf-springs *A* & *B*. For relatively small deflections, the rotational comb-drive will rotate around the common virtual pivot. Reinforcement *F*, is a folded leaf-spring, supporting the comb shuttle in out-of-plane direction, and leaving the other degrees of freedom compliant.

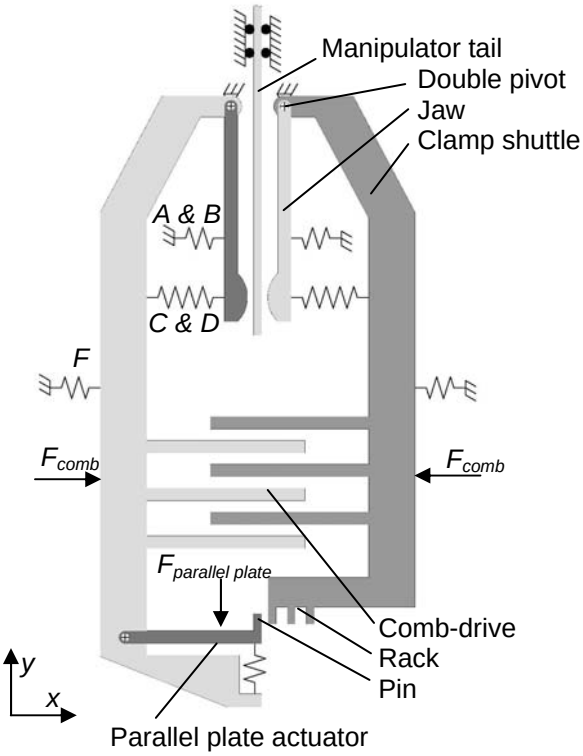

FIGURE 1. Schematic view of the clamp mechanism. The compliance of leaf-springs A, B, C, D and F are represented by 1D springs. The virtual pivots are represented by real pivots.

During the first 1.64° rotation of the jaw and 1.87° rotation of the comb-drive, the comb-drive energy is stored in leaf-springs *A, B, C, D* and reinforcement *F*, as the jaw does not touch the manipulator tail. After the jaw touches the manipulator tail the clamp comb-drive energy is mainly stored in leaf-springs *C, D* and reinforcement *F*. At the same time the clamp force starts to build up over a 0.49° clamp actuator stroke. Once a desirable clamp force is obtained, the parallel plate actuator can be gradually switched off, raising the pin in the rack. The clamp comb-drive can now be switched off. There will be some backlash due to movement of the pin in the rack until a stop is reached. Details of first generation clamping and fixation mechanism can be found in previous work [2]. The fixation mechanism freezes the clamp force without the necessity of sustaining an electrical field. The combination of the position uncertainty due to backlash of the pin in the rack and the fabrication uncertainty should not lead to considerable clamp force loss. Therefore the bending compliance of leaf-springs *C, D* and reinforcement *F* will allow pre-tension to be built up. Making the leaf-springs too compliant will require extra stroke and actuator energy for the comb-drive. Making leaf-springs too stiff leads to unacceptable loss of clamp force when locking.

Because of large clamp forces, and therefore the risk of buckling, the relatively long and slender leaf-springs *A* & *B* are loaded with a tensile force during clamping. Leaf-springs *A, B, C,* & *D* are initially pre-curved so that at the maximum overlap of the comb-fingers, the deformation causes them to be straight. Exactly
at this point the electrostatic pull-in force is greatest, and the leaf-spring's longitudinal stiffness is largest.

In order to minimize the parasitic influence of clamping on the manipulator position several measures have been taken: First, the virtual pivot is located in the middle of the manipulator-tail. Therefore nearly pure motion in *x*-direction of the jaw results, leaving the manipulator position unaffected. Second, the clamping force results in a tensile elongation of leaf-springs *A* and *B*. The leaf-spring tensile stiffnesses are tuned so the clamp force will result almost solemnly in an *x*- displacement of the jaw. The residual *y*-displacement due to the above mentioned effect is less than 1 nm. The manipulator-tail is compliant in *x*-direction to obtain an equal distribution of the clamp force in the jaws. The Hertzian contact stress due to clamping of the manipulator-tail results in an elongation of the tail of 0.19 nm in *y*-direction, which is considered to be insignificant. Consequently by clamping, the position of the manipulator will only be affected on a sub-nanometer scale.

The mechanism consists of several actuators. One actuator is used to create a controllable clamp force, the second actuator is much smaller and locks the position of the first actuator. The jaw has to build up the 0.5 mN clamp force in such a way that the manipulator position is not altered. The combination of a small locking mechanism and a larger controllable clamp actuator offers a relatively small clamping device. A comb-drive actuator is capable of realizing enough force if a transmission ratio is used. Comb-drive actuators deliver controllable force output and are relatively easy to manufacture. The applied clamp comb-drive has 144 comb-finger pairs and delivers a torque of 52nNm at 80V, which is equal to 97μN at the middle of the comb. The longest comb-fingers are 93 μm long and 3 μm wide. According to Elata [3] this geometry will not result in finger pull-in at 80V. The symmetric design of the two combs interacting results in mostly similar geometric displacements with respect to the *y*-direction, which is beneficial for the alignment of the combs fingers.

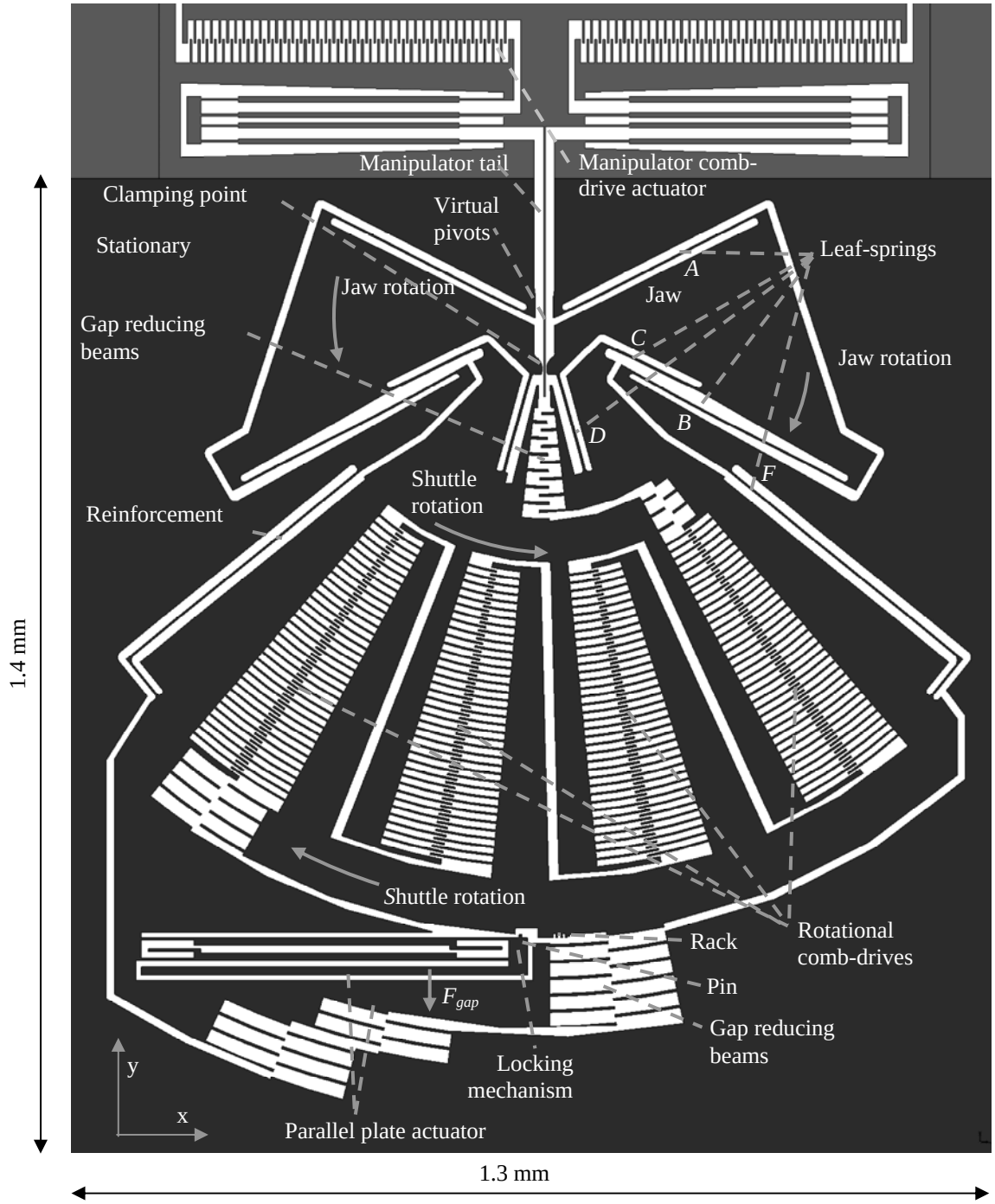

FIGURE 2. The clamp design with part of the manipulator comb-drive actuator

Results obtained from modeling [2] show that 33% of the comb-drive force and 79% of the stroke is necessary for closing the 2 μm gap between the manipulator tail and the jaw. This gap is constrained by the process. The stiffness in *y*-direction of the jaw at the virtual pivot is 4.1 10^4 N/m, caused by the large tensile stiffness of leaf-springs *A* and *B*. Loading the jaw with the maximum force of the manipulator comb-drive results in 12 nm manipulator actuator movement. The highest stress occurs in leaf-spring *D*, mainly due to bending, and reaches 405 10^6 N/m^2. The calculated lowest natural frequency of the system not clamping the manipulator tail is 2.3 kHz. The associated vibration mode is a rigid body rotation of the comb-drive with jaw around the virtual pivot.

Process

The process implemented is based on the three mask process of the back side release process demonstrated by Sarajlic [4]. It offers a 35 μm thick structural layer, and a 3-20μm trench width design freedom. The fabrication is compatible with the fabrication of the parallel kinematic manipulator process.

First insulation trenches are installed in the wafer [5]. A 35 μm thick membrane is created by backside KOH etching. The mechanical structures are etched by a Bosch recipe up to 90% of the membrane depth. Etching the last 10%, the release of these suspended structures, needs consideration. Basically there are two types of release etching: releasing by directional etching or by isotropic etching. Directional etching creates heat in the suspended devices. Although helium back-side cooling by a dummy wafer is being used, this energy has to flow through the leaf-springs, which easily break-down. In Figure 3a and 3b for example the resist has been overheated. In this case the device however is still intact. Using an isotropic release from the front or back side introduces much less heat, however it calls for the release to be confined in a short time span. The chemical etching will deteriorate the side wall passivation of devices and in the end it etches the devices themselves. In all cases the thickness of the membrane, the depth of the Bosch-like etching and the last release etching step should be uniform over the wafer area.

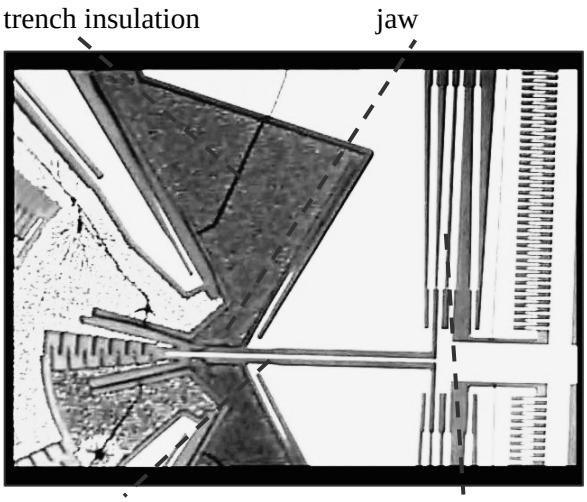

FIGURE 3a. The manipulator actuator is activated.

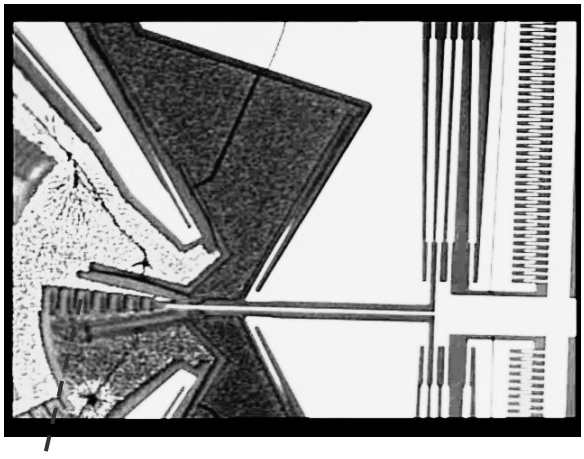

FIGURE 3b. The jaw clamps the manipulator tail.

Figure 3a and 3b show a released clamp with test actuator. In Figure 3a the test actuator has been switched on and the folded flexures are deflected. In Figure 3b the manipulator tail has been clamped between the jaws. At present no detailed characterization has been performed.

CONCLUSION

A clamp is proposed for a micro-machined high-precision large force clamping mechanism. It includes an un-powered mechanical locking system to maintain the clamping force at 0.5 mN. Although compliant mechanism design in MEMS design requires extra attention because of the relatively large deflections, small actuations forces and relatively large actuation stiffness, the real challenge lays in designing within the limited fabrication techniques. Though still in development, the fabrication technique proposed offers 35 μm high mechanisms with a trench width bandwidth of 3-20μm. The fabrication technique is compatible with the fabrication of a 6 Degree-of-freedom manipulator.

REFERENCES

1. D.M. Brouwer, B.R. de Jong, H.M.J.R. Soemers, 2006, MEMS-based 6 Degrees-of-freedom parallel kinematic precision micro manipulator, Proc. of EUSPEN int. conf, 6: 111-114.
2. D.M. Brouwer, B.R. de Jong, H.M.J.R. Soemers, J. Van Dijk, 2006, Sub-nanometer stable precision MEMS clamping mechanism maintaining clamp force un-powered for TEM application, Journal of Micromechanics and Microengineering, Vol.16, No. 6: 7-12
3. D. Elata, V. Leus, 2005, How slender can comb-drive fingers be, J. Micromech. Microeng., 15: 1055-1059.
4. E. Sarajlic, 2005, Electrostatic microactuators fabricated by vertical trench isolation, Ph.D thesis, University of Twente, Enschede, The Netherlands.
5. G Yan, Y Zhu, Z Wang, R Zhang, Z Chen, X Liu and Y. Wang, 2004, Integrated bulk-micromachined gyroscope using deep trench isolation technology, Int. Conf. on Micro Electro Mechanical Systems MEMS, Maastricht, The Netherlands: 605-608.